A Continuously Renewed Copper Electrode For Constant-Potential Amperometry

A Thesis

Presented to

The Faculty of the Department of Chemistry and Biochemistry

University of Texas at Arlington

In Partial Fulfillment

of the Requirements for the Degree of

Master of Science in Chemistry

December 2022

By

Andrew Franklin

Arlington, Texas

Abstract.

Pulsed amperometric detection (PAD) is a well-established technique used for the detection of electroactive compounds following Ion Chromatography (IC). Target analytes, such as carbohydrates and amino acids, typically have no suitable chromophores and are not detectable by suppressed conductivity following IC separation. While direct current (DC) amperometry is simpler, the formation of oxidation products quickly fouls the electrode surface; PAD removes these products extending electrode longevity for up to ~2 weeks of operation. To further extend electrode lifespans, a new strategy is introduced herein using DC amperometry on a sacrificial copper wire anode. The wire face continually dissolves under oxidative conditions while a spring-loaded plunger feeds the wire into a cell so that the interelectrode distance between the wire working electrode (WE) and counter electrode (CE) is maintained. High nanomolar (sub-ppm) limits of detection have been quantified for simple sugars, and with the use of internal standards the electrode has demonstrated virtually no loss of signal over 2 weeks of continual operation.

Table of Contents

Abstract ii

Table of Contents iii

List of Figures iv

Chapter 1 (Introduction) 1

Pulsed amperometric detection (PAD) 1

HPAE chromatography and detection of carbohydrates 2

Copper electrodes 3

Chapter 2 (Experimental) 6

Materials 6

Chromatographic instrumentation 6

Design of continuously renewed copper electrode 7

Preparation of copper working electrode 10

Working voltage optimization 10

Electrode longevity 11

Chapter 3 (Results and Discussion) 12

DC amperometry vs. PAD 12

Working voltage optimization 14

Electrode longevity 16

Flow distributors vs. outlet shim 18

Chapter 4 (Conclusions) 22

References 23

Appendix 25

List of Figures

Figure 1. Continuously renewed electrode schematic in the flow distributor configuration. Clockwise starting at the plunger: the plunger is made from a spring-loaded, blunted tungsten carbide drill bit with a tip diameter ~0.8 mm; the WE is comprised of a 0.8 mm diameter BNC cable copper core; gaskets are custom cut from Viton (fluorocarbon) tubing – one has 1/8" o.d. and seals at the face of the sheath tubing, the other 1/16" o.d. and sealed at the face of the (green) PEEK tubing; spacers were cut from 1/16" o.d. x 0.0025" i.d. PEEK tubing; the CE is formed by a 1/16" o.d. x 0.004" i.d. stainless steel tube; flow distributors were custom cut from 5-mil Kapton (polyimide) and have i.d.'s larger than the diameter of the copper WE; finally the sheath tubing had 1/8" o.d., 1/16" i.d. and was used for alignment and to allow better Kapton component fabrication.

Figure 2. Schematic of the electrode with the flow distributors replaced with a single piece of 5-mil Kapton with an outlet slit cut. The outlet shim had a 1/8" o.d. x 0.25 mm i.d. All other components were the same as described in Figure 1.

Figure 3. A copper electrode in the outlet shim geometry in a constant stream of 60 mM KOH at 60 μL/min. The electrode had equilibrated to +0.5 V prior to the initial step to +0.6 V. Each step was given ~30 min to decay. The cut-out highlights the copper oxide equilibrium induced decay that dominates the baseline after the initial electrical double layer decay.

Figure 4. Limits of detection of glucose, fructose, and sucrose as separated in 60 mM KOH at 60 μL/min on a CarboPac200 column. Data points displayed were experimentally determined from peak heights and average noise (74 pA). Trends displayed are 3rd order polynomials fit to limits of detection vs detector voltage. LODs are as follows: glucose = 0.79 μM (0.14 ppm), fructose = 0.97 μM (0.17 ppm), sucrose = 1.17 μM (0.40 ppm).

Figure 5. Peak heights over two weeks for inulin peak at t_R = 31.6. In blue are normalized peak heights; in orange the peak heights have been divided by peak heights from peaks at t_R = 30.2 (treating this peak as an internal standard). The maximum observed rate of change of peak heights was 0.29 %/hr. Noise was virtually invariant over this time, so with the application of an internal standard S/N was essentially constant for the 14 days observed.

Figure 6. Sample baseline corrected and normalized inulin separations comparing the flow distributor and outlet shim geometries. In the flow distributor configuration an unusual fronting was apparent on the early eluting peaks, progressively becoming less pronounced as the separation proceeded. The outlet shim configuration resolved this problem and allowed the detection of previously unresolved

shoulder peaks. This outlet shim separation is what would be expected from a separation using a commercial gold electrode for detection.

Figure 7. 10 ppm fructose flow injections in 60 mM KOH at 60 μL/min. Red and blue traces are peaks detected by constant-potential amperometry on a copper electrode; the green trace was detected used PAD with a commercial gold electrode. All peaks have been baseline offset and normalized for comparison. The gold electrode uses a pulsed waveform that includes a negative component creating a distinct "elbow" around t = 0.2 min. This elbow makes tailing incomparable between peaks. By instead comparing peak widths at half their maxima, it is apparent that in the flow distributor configuration the detector has induced dispersion.

Appendix 1. Inulin separation as observed with the flow distributor configuration. Separations were performed at 60 μL/min on a CarboPac200 column. Potassium methanesulfonate (KMSA) began at 40 mM, was ramped to 160 mM over 45 minutes, then held constant for 5 minutes. KOH began at 70 mM, was decreased to 20 mM over 45 minutes, then held constant for 5 minutes. Afterwards KOH was increased to 140 mM to regenerate the column, then decreased to 70 mM to re-equilibrate for the next injection.

Chapter 1

Introduction

Pulsed amperometric detection (PAD).

Pulsed amperometric detection (PAD) is a popular technique used to clean electrode surfaces between periods of detection. This is done by detecting at a given potential, followed by brief periods of highly positive or negative potentials to desorb detection products. For instance, a standard triple-potential waveform covering a one second span using a gold WE may proceed as follows: a constant detection potential of +0.05 V for 400 ms which is then rapidly (10 ms) increased to +0.75 V and held constant for 200 ms, then rapidly decreased below detection potentials to -0.15 V and held constant for 400 ms, then rapidly returned to detection potentials.[1,2] In this form the highly positive potential oxidizes the electrode surface and desorbs any detection products. The subsequent negative potential reduces the oxide layer formed by the positive pulse, thus renewing the electrode surface.

During the oxidative step some material is lost, leading to electrode recession and eventual signal decay. The electrode must then be removed from the system and repolished before reinserting and recalibrating. To reduce the downtime and irreproducibility associated with manual electrode polishing, disposable thin film electrodes were introduced as well as a new quadruple-potential waveform. Because the electrode is only a few micron thick, it rapidly dissolves from the plastic substrate under highly oxidizing conditions; the new waveform then using a strongly reducing pulse to desorb analytes.[2] Such a waveform may proceed as: 1) Integration +0.1 V, 400

ms, 2) reduction -2.0 V, 20 ms, 3) oxidation, +0.6 V, 10 ms, and 4) reequilibration, -0.1 V, 70 ms. This minimized period of positive voltage reduces electrode oxidation and subsequent dissolution. However, even with these waveform improvements, electrodes will still dissolve/recede over time.[3]

HPAE chromatography and detection of carbohydrates.

Carbohydrates have been a historically challenging class of analytes to separate and quantify in low concentrations. Legacy analysis methods include: pre-column derivatization to improve volatility for gas chromatography [4]; high capacity, acidic, metal form cation exchange chromatography [5]; and borate derivation for borate-complex anion exchange chromatography [6]. Each were constrained by lengthy analysis times and other technique specific limitations such as peak broadening, limited selectivity, solvent restrictions, and necessarily low flow rates.[7] RPHPLC has also been coupled with refractometry to analyze carbohydrates, but refractive index measurements limit gradient elution and are comparatively insensitive. However, reducing sugar interactions with amine-functionalized stationary phases impaired column efficiency. Other stationary phases have been studied, but they experienced limited resolution in early eluting peaks or limited selectivity.[8,9]

Rocklin and Pohl first reported the use of high performance anion exchange chromatography (HPAEC) in 1983 as a rapid, underivatized separation method compatible with electrochemical detection (previous LC methods were restricted to UV-Vis absorbance or refractive index detection).[7] Anion exchange chromatography had previously been incompatible with carbohydrate analysis because the basic eluents

dissolved the silica stationary phases; this was resolved with the development of polymer-based stationary phases.[10] HPAEC separates carbohydrates by their weakly acidic nature and offers control over retention times and elution order by simply changing eluent strength and column temperature.[7] In their 1983 study, Rocklin and Pohl used a gold working electrode to test both constant-potential amperometry and PAD; they found PAD to be the more reproducible and long-lived mode of detection as the constant-potential caused oxidized analyte build up. Conversely, PAD used a repeated pattern of three voltages to clean the electrode surface between detection periods, extending electrode longevity. Using this pulsed waveform with a gold electrode, Rocklin and Pohl were able to detect monosaccharides in concentrations as low as 30 ppb.

Copper electrodes.

Copper electrodes have been studied as an alternative to gold and platinum electrodes for post-column detection since at least the late 70s.[11] Loscombe et al. used a copper ion-selective copper electrode for post-column voltametric detection based on a copper sulfate reaction with 5 amino acids separated under reverse-phase conditions. Interestingly, they found that the copper electrode responded without the copper reactant, albeit at the cost of longevity (signal was restored by polishing). Kok et al. used a copper electrode in a constant potential mode for post-column amperometric detection, sans the copper reactant, and found that by mildly pre-oxidizing the electrode detection limits of amino acids were comparable to that of ninhydrin derived UV absorbance.[12] Kok et al. also attributed their electrode's performance and longevity to a

constant renewal of the copper oxide electrode surface induced by dissolution into the surrounding media. Other groups have similarly used constant-potential copper electrodes for amperometric detection of carbohydrates and found pre-oxidation beneficial for sensitivity and longevity, as well as having demonstrated superior signal-to-noise ratios (S/N) by using copper as opposed to similar 8B and 1B transition metals.[13,14]

It is known that in alkaline media (such as the eluents typically used in anion exchange chromatography) these copper electrodes operate in a complex equilibrium between elemental copper, Cu (I), Cu (II), and some authors suggest that at higher voltages (> +0.6 V vs Ag/AgCl) Cu(III) may evolve.[13,15] These copper cations may act as chelating agents or oxidants, or the analytes may adsorb to the copper oxide surface of the electrode and be catalytically oxidized.[15] When analytes are adsorbed to the electrode's surface, the copper oxide surface catalyzes analyte oxidation. Because of this copper cation equilibrium, different analyte species will respond to the same detector at different rates based on copper oxide distribution (a function of voltage and electrode history) and analyte ionization constants.[15] Regardless of the exact mechanism of detection, copper electrodes have been found to perform more sensitively, and stably, than other transition metals when used in a constant potential mode.[13,14]

Copper electrodes' sensitivity and stability have previously been compared to those of other transition metals electrodes operated in a constant potential mode such as gold, platinum, and nickel.[14] Luo et al. found that glucose could be detected as low as 30 nM on a copper electrode operated at +0.58 V vs Ag/AgCl whereas platinum at

+0.50 V could only detect as low as 200 nM. They also found that under optimum conditions a copper electrode operated continuously in a constant-potential mode was usable for up to 2 weeks before repolishing was necessary. The long-lived nature of their copper electrode can be explained by Kok et al.'s findings that the copper oxide or hydroxide layer was continually dissolving under alkaline conditions at cell potentials > +0.1 V. This copper oxide equilibrium results in the electrode face being constantly renewed, thus unmarred. Kano et al. found that by mildly oxidizing their copper electrode before operation, signals would be stabilized faster and LODs were nearly constant over two weeks. Furthermore, Luo et al. and Ueda et al. independently found that copper electrodes had the most favorable S/N.[14,16]

Chapter 2

Experimental

Materials.

All aqueous solutions were prepared using water filtered through an Aries-1102D High-Purity D.I. Loop. A 1000 ppm aqueous solution containing equal mass concentrations of anhydrous D-glucose (Mallinckrodt), D-(-)-fructose (Baker Analyzed Biochemical), and sucrose (Fisher Scientific) was prepared as stock solution and subsequently diluted. Order of magnitude serial dilutions were performed down to 10 ppb. These solutions are hereinafter referred to as GFS solutions. A separate aqueous solution of 5000 ppm inulin from chicory extract (Sigma Aldrich) was prepared and stored at 9 °C. All solutions were prepared in 100 mM sodium azide. All samples were injected in 400 nL aliquots.

Chromatographic Instrumentation

Analytes were separated on an anion exchange CarboPac PA200 guard (50 x 0.4 mm I.D.) and separation (250 x 1 mm I.D.) column set with a Dionex ICS-5000. The column was housed in a 35 °C thermostated compartment. Dual eluent generators (KOH and methanesulfonic acid) were used to produce carbonate-free eluents. Cell potentials were generated by an ICS-5000 electrochemical module (P/N 072043) and Ag/AgCl reference electrode. System control and data acquisition were performed using Chromeleon v7.2. All the above were provided by Dionex, Sunnyvale, CA.

Design of Continuously Renewed Copper Electrode.

The cell was configured so that eluent impinged upon a continuously advanced working electrode (WE), similar to a spring-loaded check valve. When a sufficiently large voltage was applied to a WE in the presence of alkaline media, an oxide layer formed on the electrode's surface. This oxide layer itself was soluble in the alkaline media, so overtime the surface of the WE oxidized and dissolved. To compensate for dissolution, the WE was continuously repositioned by a spring-loaded tungsten carbide plunger.

All tubing were housed in 1/8" o.d. x 1/16" i.d. PTFE jacket tubing for alignment and ease of use. The CE was formed from a 1/16" o.d. x 0.004" i.d. stainless-steel tube that entered a tee cell. An insulating polymeric spacer (1/16" o.d. x 0.0025" i.d. cut from PEEK chromatography tubing) was placed between the 0.8 mm diameter copper WE and stainless-steel CE to prevent electrical contact. An older design of this cell relied on aligning the interface of a silicone septum and an insulating spacer with a hole drilled into the jacket tubing to allow eluent to reach the outlet.[Wilson2021] This interface alignment proved prone to blocking and difficult to reproduce, so herein the cell's outlet has been operated in two different geometries: one which relies on four, 5-mil thick Kapton flow distributors to create a series of leaky interfaces so eluent could reach the outlet (Fig. X); the other configuration used a single piece of 5-mil Kapton shim with an outlet slit cut into it (Fig. X+1). In the case of the flow distributors, the i.d. was sufficiently large so that the electrode walls were encapsulated in eluent (e.g. 1 mm i.d. for a 0.8 mm dia. copper wire). Furthermore, the previous design relied on compressed air to drive the plunger; the compressed air feed has been removed, as there were persistent leaks around the plunger, and replaced with a spring to ensure constant advancement.

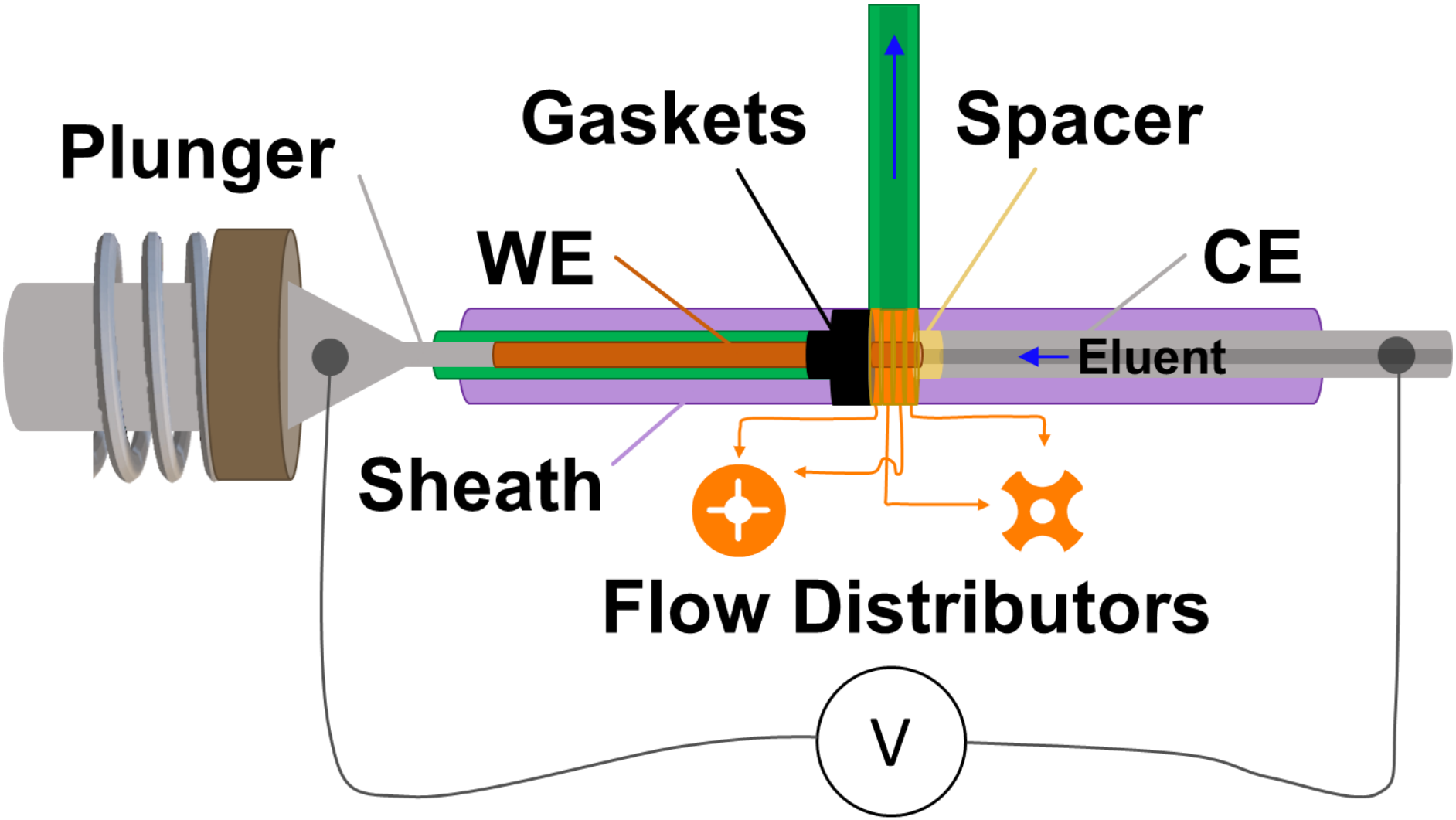

Figure 1. Continuously renewed electrode schematic in the flow distributor configuration. Clockwise starting at the plunger: the plunger is made from a spring-loaded, blunted tungsten carbide drill bit with a tip diameter ~0.8 mm; the WE is comprised of a 0.8 mm diameter BNC cable copper core; gaskets are custom cut from Viton (fluorocarbon) tubing – one has 1/8" o.d. and seals at the face of the sheath tubing, the other 1/16" o.d. and sealed at the face of the (green) PEEK tubing; spacers were cut from 1/16" o.d. x 0.0025" i.d. PEEK tubing; the CE is formed by a 1/16" o.d. x 0.004" i.d. stainless steel tube; flow distributors were custom cut from 5-mil Kapton (polyimide) and have i.d.'s larger than the diameter of the copper WE; finally the sheath tubing had 1/8" o.d., 1/16" i.d. and was used for alignment and to allow better Kapton component fabrication.

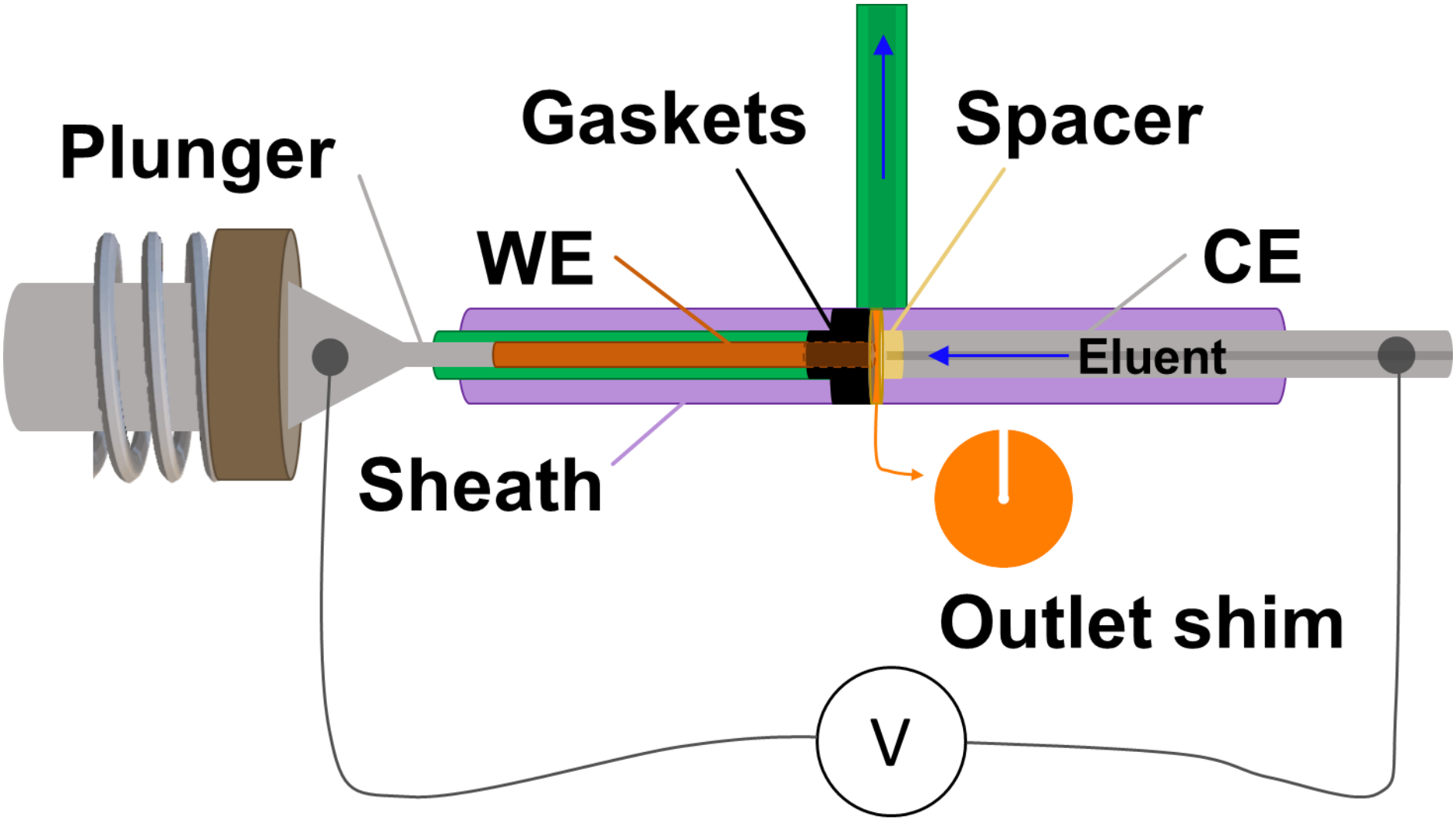

Figure 2. Schematic of the electrode with the flow distributors replaced with a single piece of 5-mil Kapton with an outlet slit cut. The outlet shim had a 1/8" o.d. x 0.25 mm i.d. All other components were the same as described in Figure 1.

Preparation of Copper Working Electrode.

Unless specified otherwise, all potentials herein are vs Ag/AgCl. Prior to analyte detection, each copper WE was oxidized with DC potentials (see details below) in 60 mM KOH flowing at 60 μL/min. Electrode potentials were stepped in +100 mV increments from 0 to +1.0 V. A sharp increase in current was observed after each step, followed immediately by a decay. This decay occurs rapidly at first (1-5 minutes) followed by a slow period (20-30 minutes) of additional decay. The rapid portion of decay is likely due to capacitive discharge of the electrical double layer at the electrode's surface, where the slower decay is from copper oxide equilibration under new conditions. Each step was allowed to decay until the rate of decay had decreased to <200 pA/s, typically ~30 minutes. Finally, each working electrode was held at +1.0 V in the aforementioned eluent stream for at least 16 hours before any injections were performed.

Working Voltage Optimization

A copper electrode was prepared as described above and installed on the ICS-5000. Each sample was separated isocratically on the PA2000 column at 60 μL/min in 60 mM KOH. 10 ppb – 1000 ppm GFS samples were injected in quintuplicate with detector potentials stepped in 50 mV increments from +0.5 – 1.05 V vs Ag/AgCl. Samples were analyzed in triplicate after sufficient time had passed for the baseline to equilibrate to each new voltage. The detector's performance was evaluated at each potential based on peak heights, areas, peak widths, background current, and noise as measured over a 10 second window.

Electrode Longevity

Inulin samples were filtered with a 1.2 μm Nylon syringe filter before injection. Inulin samples were separated by gradient eluent in a dual KOH/KMSA solution (see Appendix 1). The same inulin solution was injected and separated repeatedly for two weeks to evaluate detector longevity. Peak characteristics and baseline noise were determined in the same way as described in “Working Voltage Optimization”.

Chapter 3

Results and Discussion

DC Amperometry vs. PAD.

As demonstrated in Wilson's thesis, standard gold electrodes are incompatible with DC amperometry due to near immediate signal degradation induced by electrode consumption.[17] To this end, a pulsed quadruple-waveform is appealing to use with a copper working electrode. However, between the electrical double layer capacitively discharging at the electrode's surface and oxide equilibria reestablishing after each change in potential, a substantial decay pattern limited response time. This is visualized below in Figure X where the copper electrode was stepped in +100 mV increments in 60 mM KOH flowing at 60 μL/min. Each step was held for ~30 minutes and can be considered in two parts as a rapid capacitive decay followed by a slow equilibria establishment. The capacitive decay is formed by the short-lived (>2 min) peak induced the moment electrode potential is changed. The copper oxide equilibria decay is seen in the cut-out in Figure X and can take 20-30 minutes to establish. Furthermore, even after the electrode had been conditioned for analysis, this capacitive decay continued to be observed regardless of if the voltage was stepped positive or negative (a typical gold electrode using a quad-waveform will pulse negative to remove oxide buildup). Because of these limitations, these copper electrodes have only been successfully operated in a constant-potential mode.

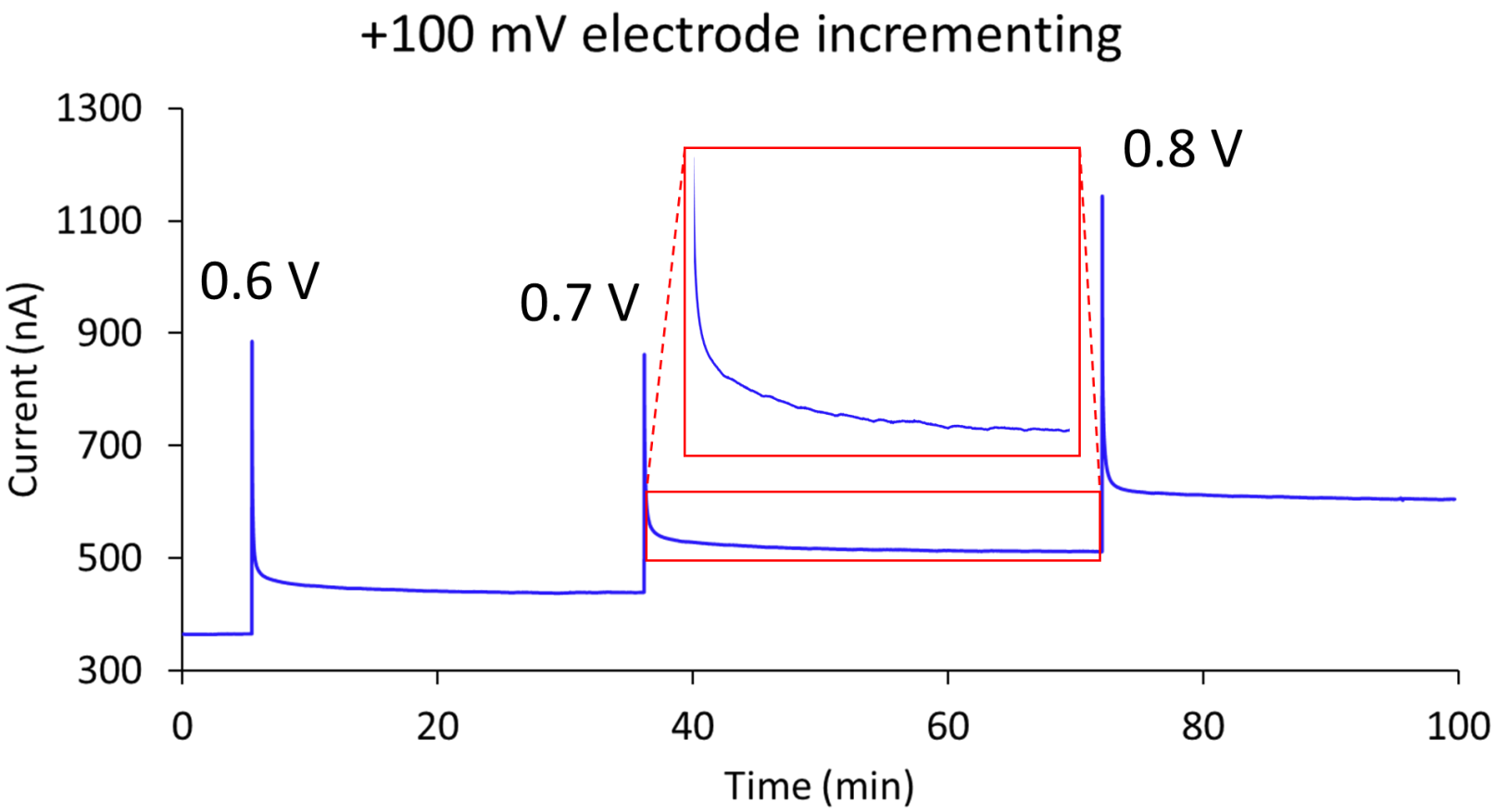

Figure 3. A copper electrode in the outlet shim geometry in a constant stream of 60 mM KOH at 60 μL/min. The electrode had equilibrated to +0.5 V prior to the initial step to +0.6 V. Each step was given ~30 min to decay. The cut-out highlights the copper oxide equilibrium induced decay that dominates the baseline after the initial electrical double layer decay.

Working Voltage Optimization.

Optimal operating voltages were determined using GFS solutions as model analytes. Voltages >1.05 V were not evaluated because electrode damage was observed at potentials above 1.05 V. Peak heights and noise were calculated with a custom LabView program. Noise was measured over a 10 s span in a region before the void; drift was first corrected for before standard deviation was calculated from the corrected baseline. The noise was independent of the applied voltage: A linear correlation of noise versus voltage resulted in a R^2 of 0.0052. Not surprisingly, the intercept accounted for 87 % of the average noise (74 pA). Because of virtual constancy of the noise, signal-to-noise ratios as a function of voltage were determined using an average noise.

3rd order polynomial fits for LOD vs voltage were used to generate the trendlines shown in Figure X and to determine their optimal voltages. Across all GFS concentrations, optimal voltages for glucose, fructose, and sucrose were found to respectively be 1.000 ± 0.008 V, 0.979 ± 0.001 V, and 1.003 ± 0.011 V. At these voltages, LODs for glucose, fructose, and sucrose were found to be 0.14 ppm (0.79 μM), 0.17 ppm (0.97 μM), and 0.40 ppm (1.17 μM) respectively. Limits of detection were comparable on a molar basis; differences were due to the broadening and diluting of the later eluting peaks as seen in Figure X. At low concentrations (1 ppm) all peak areas differed by < 15% with ± 5 % measurement error, indicating the electrode responds on a molar level for these simple sugars.

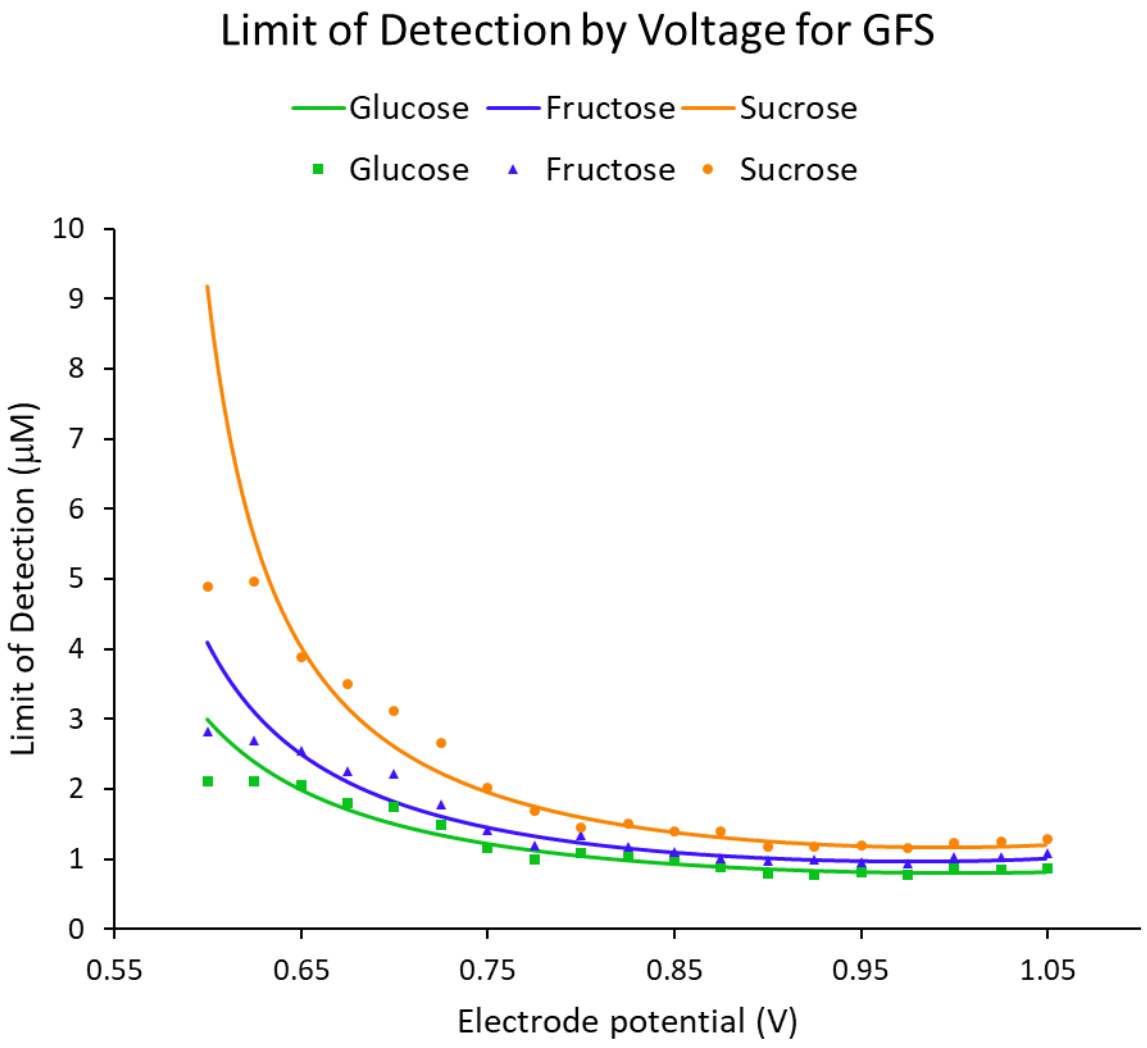

Figure 4. Limits of detection of glucose, fructose, and sucrose as separated in 60 mM KOH at 60 µL/min on a CarboPac200 column. Data points displayed were experimentally determined from peak heights and average noise (74 pA). Trends displayed are 3rd order polynomials fit to limits of detection vs detector voltage. LODs are as follows: glucose = 0.79 µM (0.14 ppm), fructose = 0.97 µM (0.17 ppm), sucrose = 1.17 µM (0.40 ppm).

Electrode Longevity.

The inulin separation produced >100 peaks spanning 50 min, seen in Appendix 1. Three sequential peaks near the middle of the chromatogram (t_R = 30.2, 30.9, 31.6 min) were chosen to calculate peak heights as models for reproducibility over time. For the first four days, during which 61 automated injections were repeatedly performed, there was essentially no change in peak height; the peaks at t_R = 30.2, 30.9, and 31.6 min, exhibited %RSDs of 0.42 %, 0.44 %, and 0.46 %, respectively. After this initial four-day period, peak heights began to drift over daylong periods though no long-term decay was observed that would suggest fouling or recession of the WE away from the CE. This drift was at a most 0.29 %/hr.

Due to the slow drift, a single internal standard peak may be used per chromatogram to improve quantitation. Treating the peak at t_R = 30.2 min as an internal standard, the %RSDs of the peaks at 30.9 and 31.6 min were found to be 0.42 and 0.64 %, respectively, for the full 14 days. Additionally, after this four-day period noise became much more scattered and %RSD of the noise increased from 14.3 % for the first 4 days to 33.2 % by 14 days. However, within this 10-day period of increased noise scatter, only 25.4 % of noise measurements fell outside of a ±3σ window from the average noise of the initial 4-day period. That is to say, the noise was largely unchanged over the 14-day period, with occasional events of increased noise. This may be resolved by the addition of external electrical shielding.

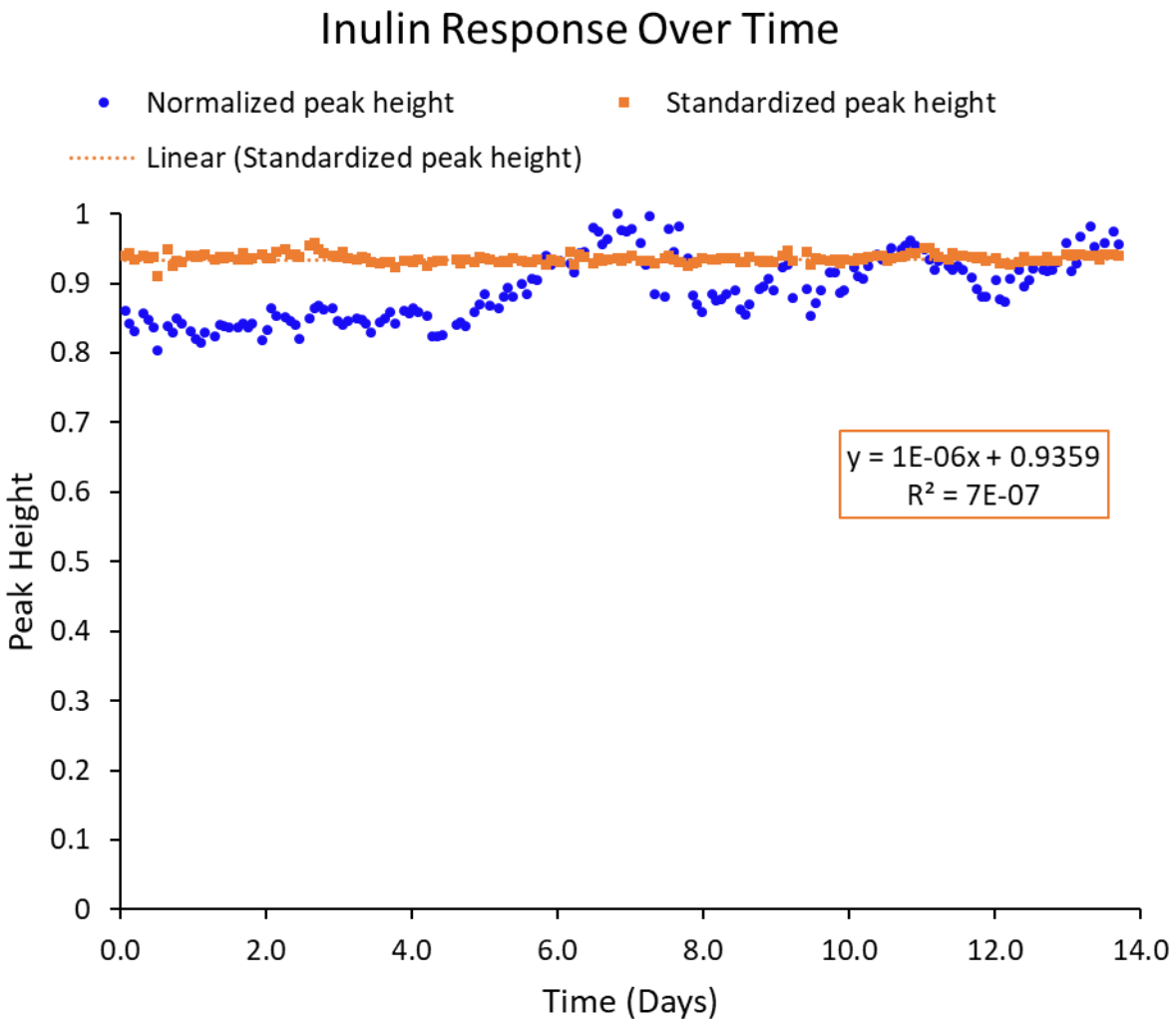

Figure 5. Peak heights over two weeks for inulin peak at t_R = 31.6. In blue are normalized peak heights; in orange the peak heights have been divided by peak heights from peaks at t_R = 30.2 (treating this peak as an internal standard). The maximum observed rate of change of peak heights was 0.29 %/hr. Noise was virtually invariant over this time, so with the application of an internal standard S/N was essentially constant for the 14 days observed.

Flow Distributors vs. Outlet Shim

The cell has been operated with two different outlet geometries. The flow distributor model, seen in Figure X, uses four 5-mil (~125 μm) thick Kapton pieces that have been cut with i.d.'s larger than that of the working electrode (e.g. a 0.8 mm electrode may have flow distributors with i.d.'s of 1.0 mm). Consequentially, the electrode walls exposed to eluent in the length of flow distributors are electrically active detection sites. Conversely, the Kapton outlet shim (seen in Figure X+1) seals on the electrode face (except for a small channel aligned to the tee exit) and limits detection to the inner diameter cut out from the Kapton shim. It should be apparent that the exposed surface areas differ between the two designs and that the stagnant zones around the flow distributor design may adversely affect dispersion, especially after switching to the larger 1/8" sheath tubing. Further, the varying distance/geometry may lead to unintended voltage drops relative to the CE and affecting the optimum working potential.

The consequence of these designs is clearly seen using complex separations, such as that of inulin from chicory root seen in Figure X, where it is impossible to resolve with the flow distributor geometry. Further, the optimum voltage for the flow distributor mode is substantially higher than that of the outlet shim (respectively, +0.975 V and ~+0.5 V). In both geometries peak height and peak area begin to decrease above their respective optima, while noise may remain constant or continue to increase with voltage. The optimum voltage for the outlet shim configuration (~+0.5V) is closer values reported in similar carbohydrate analyses with copper electrodes.[13,15] Taken together, these indicate that in the flow distributor mode the electrode overloads, and the optimum voltage is necessarily high because the analyte oxidation is sped up by the

large detecting potential. Reduced peak heights have been observed in the outlet shim configuration, but further experiments are necessary to compare the sensitivity of the two geometries.

Flow injections of 10 ppm fructose were performed to compare detector induced dispersion. Fructose was selected as the model analyte because of the three simple sugars tested, fructose demonstrated the least voltage dependency in analyte response. 400 nL injections of 10 ppm fructose were directly injected to the detector at 60 μL/min. The flow distributor configuration was operated at a constant +0.975 V, the outlet shim configuration was operated at +0.5 V, and a commercial disposable gold electrode was operated with a standard quad-potential pulsed waveform. Because the gold electrode uses a pulsed waveform that includes a reducing pulse, peak tailing between the commercial gold electrode and either copper electrode configuration were not directly comparable. This can be seen in Figure X, where the peak produced by the gold electrode has a negative step before returning to baseline. Focusing instead on peak widths at half maximum, the gold electrode had a FWHM = 2.4 s, the outlet shim copper electrode FWHM = 2.8 s, and the flow distributor configuration had a FWHM = 5.2 s. These peak widths demonstrate that in the flow distributor configuration the electrode cell has induced dispersion, where as in the outlet shim configuration the cell induced dispersion is comparable to that of a commercial gold electrode.

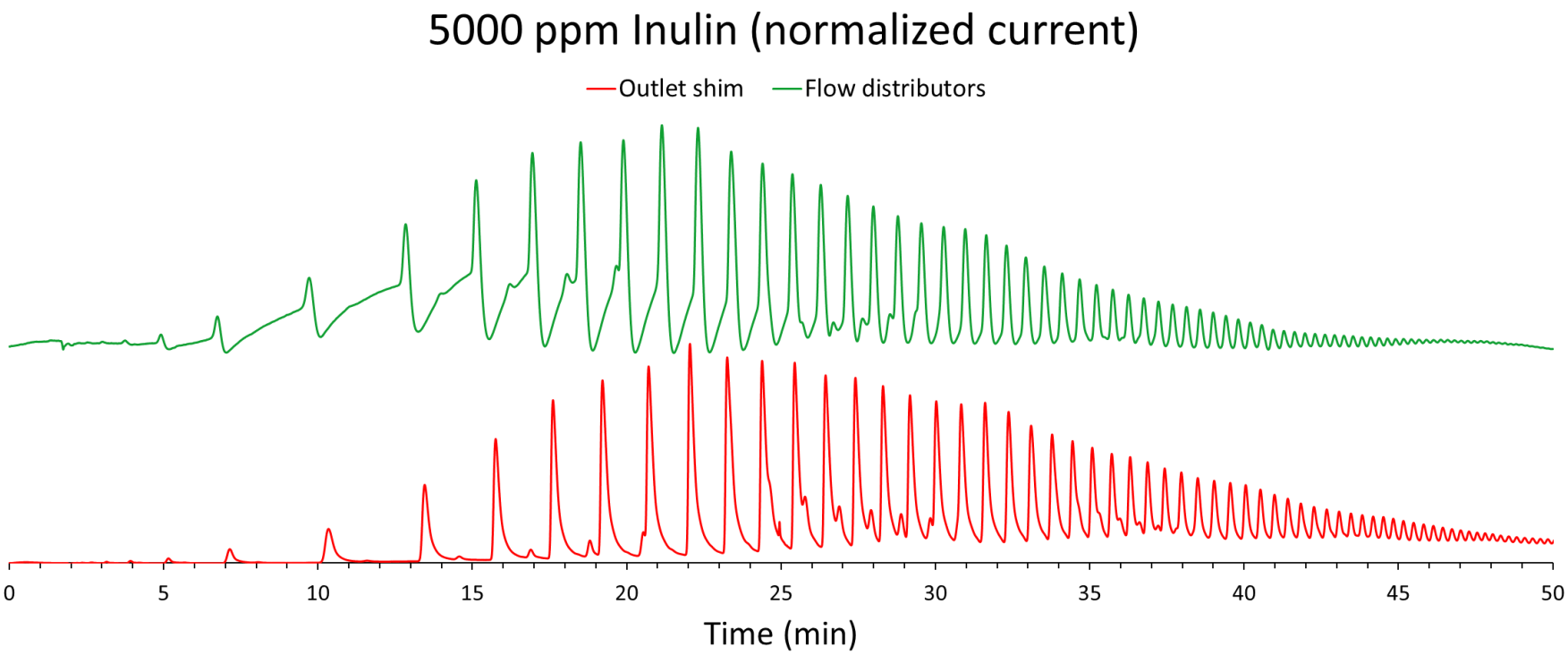

Figure 6. Sample baseline corrected and normalized inulin separations comparing the flow distributor and outlet shim geometries. In the flow distributor configuration an unusual fronting was apparent on the early eluting peaks, progressively becoming less pronounced as the separation proceeded. The outlet shim configuration resolved this problem and allowed the detection of previously unresolved shoulder peaks. This outlet shim separation is what would be expected from a separation using a commercial gold electrode for detection.

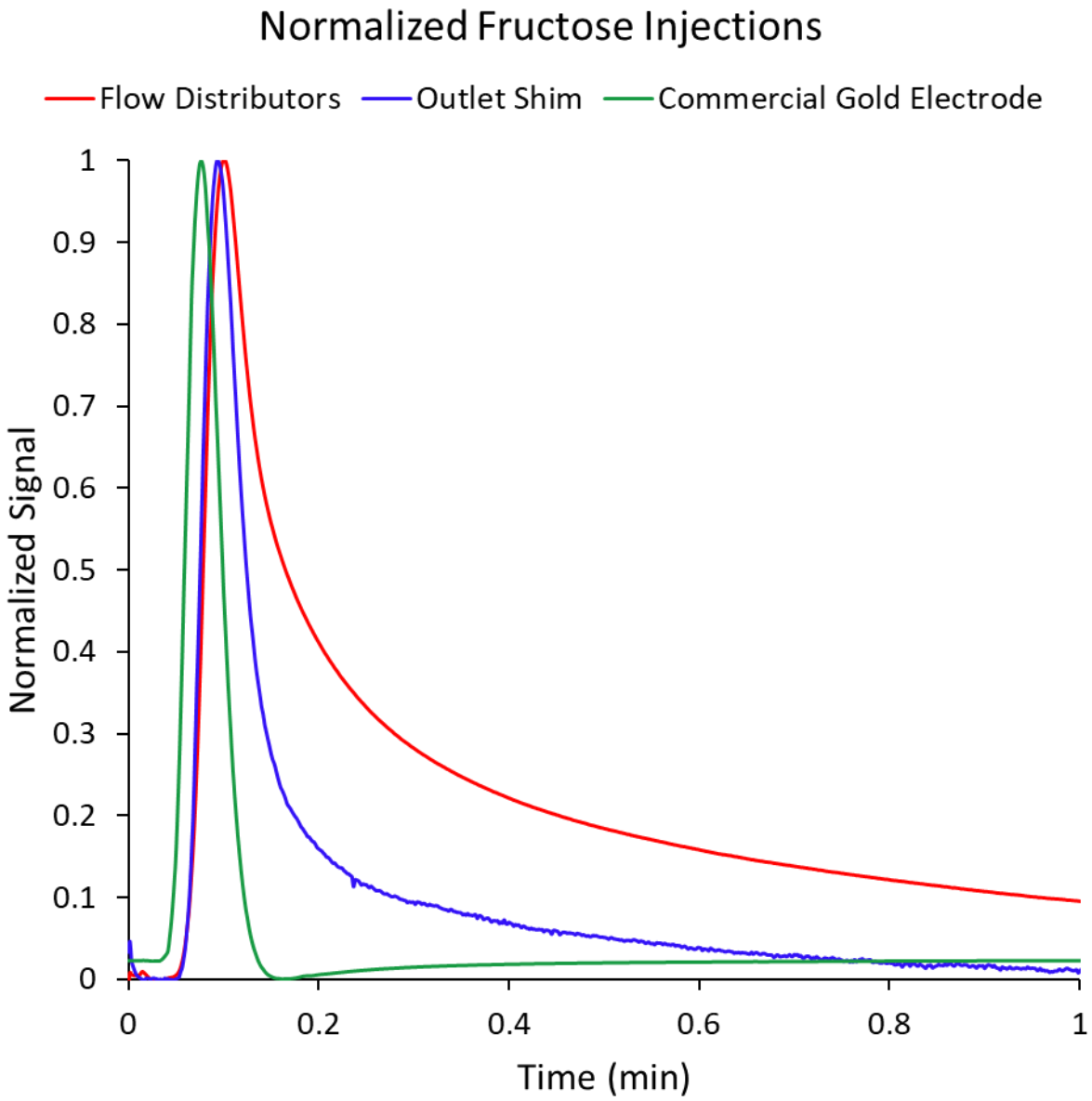

Figure 7. 10 ppm fructose flow injections in 60 mM KOH at 60 μL/min. Red and blue traces are peaks detected by constant-potential amperometry on a copper electrode; the green trace was detected used PAD with a commercial gold electrode. All peaks have been baseline offset and normalized for comparison. The gold electrode uses a pulsed waveform that includes a negative component creating a distinct "elbow" around t = 0.2 min. This elbow makes tailing incomparable between peaks. By instead comparing peak widths at half their maxima, it is apparent that in the flow distributor configuration the detector has induced dispersion.

Chapter 4

Conclusions

A copper electrode for use with constant-potential amperometry of carbohydrates has been described. The copper surface was oxidized in alkaline media, creating an equilibrium that continually dissolved the electrode's surface. This electrode was used in two geometries: one which exposed the face and walls of the electrode, the other just the face. The electrode was calibrated in each geometry with solutions containing simple sugars and was found to have maxima at +0.975 V when the electrode's walls were exposed and ~+0.5 V when only the electrode's face was exposed. Limits of detection for glucose, fructose, and sucrose were quantified for the flow distributor configuration to be <500 ppb (each sugar LOD approached 0.7 μM following order of elution). Peak widths at half heights were compared between the two electrode configurations by means of fructose flow injection; the face restricted geometry had peak widths comparable to commercial gold electrodes, while the wall exposed electrode created peaks with 50 % larger peak widths at half maximums. LODs for the face restricted geometry have not yet been determined. Response longevity was determined using inulin extract from chicory root – a pre-biotic dietary supplement comprised of a mixture of short and long chain sugars. Noise was invariant over two weeks, while peak height did drift over day-long periods. The addition of an internal standard corrects this drift, and over two weeks corrected peak heights had average %RSDs of 0.4-0.6 %. Future studies of interest include the analysis of non-carbohydrate species such as CN^-, NO_2^-, and SO_3^{2-}.

References

(1) LaCourse, W.; Johnson, D.; Optimization of Waveforms for Pulsed Amperometric Detection of Carbohydrates Based on Pulsed Voltammetry. *Anal. Chem.*, **1993**, *65*, 50-55. DOI: 10.1021/ac00049a011.

(2) Rocklin, R.D.; Clarke, A.P.; Weitzhandler, M.; Improved Long-Term Reproducibility for Pulsed Amperometric Detection of Carboyhydrates via a New Quadruple-Potential Waveform. *Anal. Chem.*, **1998**, *70*, 1496-1501. DOI: 10.1021/ac970906w

(3) Liu, Y. Dionex, Thermo Fisher Scientific, Sunnyvale, CA. Personal communication. October 2022.

(4) Knapp, D.R. *Handbook of Analytical Derivatization Reactions*, Wiley, **1979**, pp 539.

(5) Scobell, H.D.; Brobst, K.M.; Stelle, E.M.; Automated Liquid Chromatographic System For Analysis of Carbohydrate Mixtures. *Cereal Chem.*, **1977**, *54*, 905-917.

(6) Sinner, M.; Puls, J.; Non-Corrosive Dye Reagent For Detection of Reducing Sugars in Borate Complex Ion-Exchange Chromatography. *J. Chromatogr.*, **1978,** *156*, 197-204. DOI: 10.1016/S0021-9673(00)83140-4.

(7) Rocklin, R.D.; Pohl, C.A.; Determination of Carbohydrates By Anion Exchange Chromatography With Pulsed Amperometric Detection. *J. Liq. Chromatogr.*, **1983**, *6(9)*, 1577-1590. DOI: 10.1080/01483918308064876.

(8) Koizumi, K.; Utamura, T.; Okada, Y.; Analyses of homogenous D-gluco-oligosaccharides and -polysaccharides (degree of polymerization up to about 35) by high-performance liquid chromatography and thin-layer chromatography. *J. Chromatogra. A*, **1985**, *321*, 145-157. DOI: 10.1016/S0021-9673(01)90431-5.

(9) Stefansson, M.; Westerlund, D.; Ligand-exchange chromatography of carbohydrates and glycoconjugates. *J. Chromatogra. A*¸**1996**, *720(1-2)*, 127-136. DOI: 10.1016/0021-9673(95)00276-6.

(10) Cataldi, T.R.I.; Campa, C.; Benedetto, G.E.D.; Carbohydrate analysis by high-performance anion-exchange chromatography with pulsed amperometric detection: The potential is still growing. *Fresenius J. Anal. Chem.*, **2000**, *368*, 739-758. DOI: 10.1007/s002160000588.

(11) Loscombe, C.R.; Cox, G.B.; Dalziel, J.A.W.; Application of a copper electrode as a detector for high-performance liquid chromatography. *J. Chromatogr.*, **1978**, *166*, 403-410. DOI: 10.1016/S0021-9673(00)95623-1.

(12) Kok, W.T.; Brinkman, U.A.T.; Frei, R.W.; Amperometric Detection of Amino Acids in High-Performance Liquid Chromatography With A Copper Electrode. *J. Chromatogr.*, **1983**, *256*, 17-26. DOI: 10.1016/S0021-9673(01)88208-X.

(13) Kano, K.; Takagi, K.; Inoue, K.; Ikeda, T.; Ueda, T.; Copper electrodes for stable subpicomole detection of carbohydrates in high-performance liquid chromatography. *J. Chromatogr. A*, **1996**, *721*, 53-57. DOI: 10.1016/0021-9673(95)00757-1.

(14) Luo, P.; Zhang, F.; Baldwin, R.P.; Comparison of metallic electrodes for constant-potential amperometric detection of carbohydrates, amino acids and related compounds in flow systems. *Anal. Chem. Acta*, **1991**, *244*, 169-178. DOI: 10.1016/S0003-2670(00)82494-0.

(15) Marioli, J.; Kuwana, T.; Electrochemical Characterization of Carbohydrate Oxidation at Copper Electrodes. *Electrochim. Acta*, **1992**, *37*, 1187-1197. DOI: 10.1016/0013-4686(92)85055-P.

(16) Ueda, T.; Mitchell, R.; Kitamura, F.; Constant-potential amperometric detection of carbohydrates at metal electrodes in high-performance anion-exchange chromatography. *J. Chromatogr.*, **1992**, *592*, 229-237. DOI: 10.1016/0021-9673(92)85089-C.

(17) Wilson, S.R. Continuously Renewed Copper Electrode For Amperometric Measurement of Carbohydrates. MS Thesis, University of Texas Arlington, Arlington, TX, 2021. https://rc.library.uta.edu/uta-ir/handle/10106/30916 (accessed 2022-10-24).

Appendix

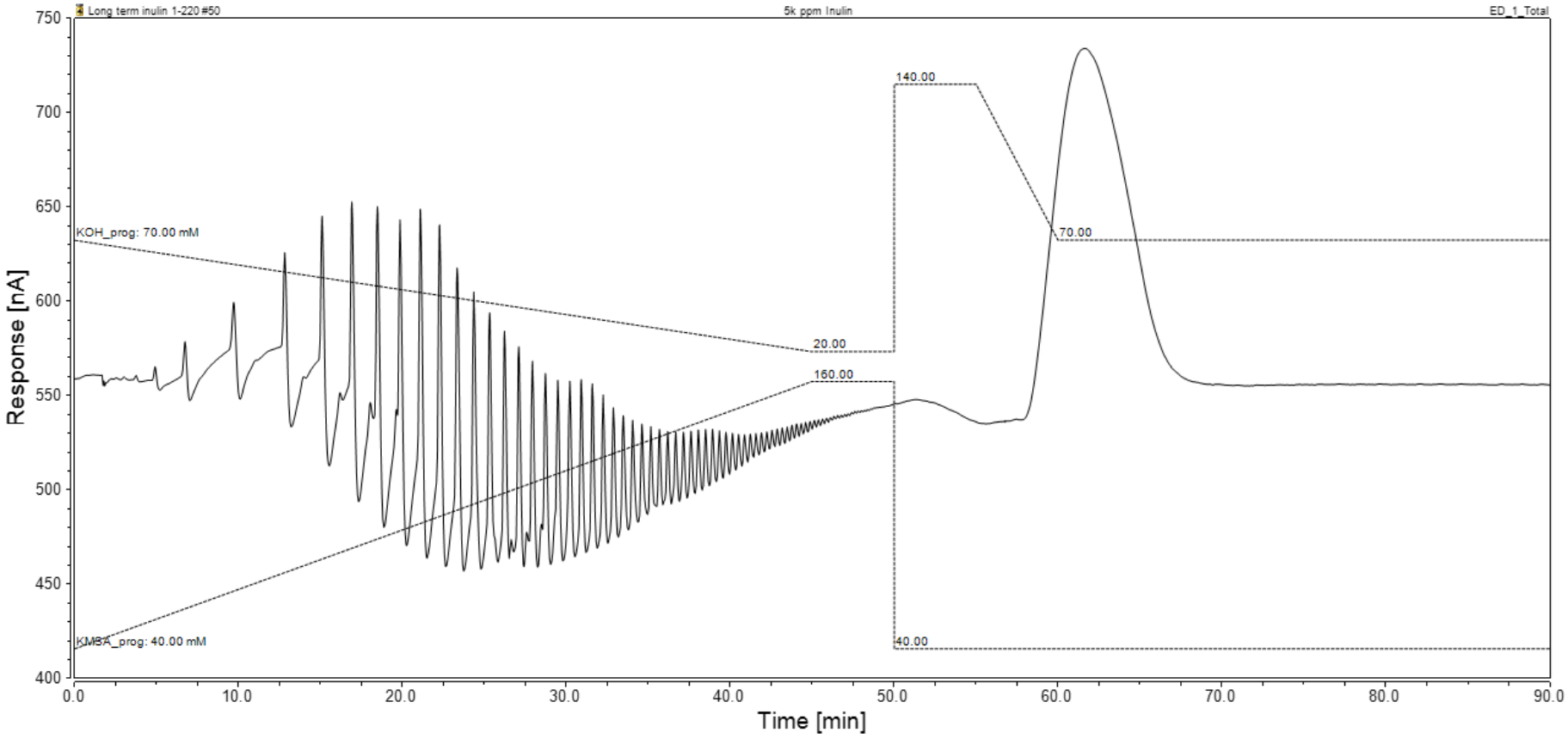

Appendix 1. Inulin separation as observed with the flow distributor configuration. Separations were performed at 60 μL/min on a CarboPac200 column. Potassium methanesulfonate (KMSA) began at 40 mM, was ramped to 160 mM over 45 minutes, then held constant for 5 minutes. KOH began at 70 mM, was decreased to 20 mM over 45 minutes, then held constant for 5 minutes. Afterwards KOH was increased to 140 mM to regenerate the column, then decreased to 70 mM to re-equilibrate for the next injection.